

GNSS Array-Aided Positioning and Attitude Determination: Real data Analyses

N. Nadarajah¹ and P. J. G. Teunissen^{1,2} and P. F. de Bakker²

¹*GNSS Research Centre, Curtin University of Technology, Perth, Australia*

²*Department of Geoscience & Remote Sensing, Delft University of Technology, Delft, The Netherlands*

Abstract

GNSS positioning and navigation have become ubiquitous with a wide variety of challenging applications including attitude determination and relative navigation. In this contribution, we analyse the performance of a novel integrated navigation method for array-aided relative positioning and attitude determination using real data. We consider two platforms equipped with multiple GNSS receivers/antennas. Precise GNSS positioning and attitude determination rely on successful resolution of the carrier phase integer ambiguities. The Multivariate Constrained-Least squares AMBIGUITY Decorrelation Adjustment (MC-LAMBDA) method is used to reliably resolve platform ambiguities making use of the knowledge of antenna geometry in the local body frame. This reliable platform processing consequently enhances the between-platform ambiguity resolution and baseline estimation. Using real data, we demonstrate that this method not only enhances the attitude determination but also improves the between-platform ambiguity resolution and the between-platform baseline estimates. Our study includes performance analyses of the array-aided positioning method in terms of number of antennas per platform, number of frequencies, and multi-GNSS vs a single system.

1 Introduction

GNSS positioning and navigation have become ubiquitous with a wide variety of challenging (terrestrial, sea, air and space) applications. Especially, GNSS-based attitude determination and relative navigation have been explored in various applications such as precision farming [1], marine navigation [2], aircraft formation flying [3], and satellite formation flying [4]. In this

contribution, we analyse the performance of a novel integrated navigation method for array-aided relative positioning and attitude determination using real data.

We consider two platforms equipped with multiple GNSS receivers/antennas. Precise GNSS positioning and attitude determination rely on successful resolution of the carrier phase integer ambiguities. The Least squares AMBIGUITY Decorrelation Adjustment (LAMBDA) method is currently the standard method for solving unconstrained GNSS ambiguity resolution problems. For unconstrained and linearly constrained GNSS models, the method is known to be optimal in the sense that it provides integer ambiguity solutions with the highest possible success-rate. The proposed method uses the multivariate constrained LAMBDA (MC-LAMBDA) method [5–9] for the estimation of platform ambiguities and attitude angles. MC-LAMBDA makes use of known antenna geometry to strengthen the underlying attitude model, enabling reliable instantaneous ambiguity resolution and attitude determination of the platforms.

The reliable estimation of platform ambiguities is consequently utilized to enhance the relative positioning of the platforms. This array-aided precise point positioning (A-PPP) method [10–12] exploits known antenna geometry of the platform to improve the underlying between-platform (baseline) model. Using real data, we demonstrate that this method not only enhances the attitude determination but also improves the between-platform ambiguity resolution and the between-platform baseline estimates. Our study includes performance analyses of the array-aided positioning method in terms of number of antennas per platform, number of frequencies, and multi-GNSS vs a single system. This contribution is organized as follows:

Section 2 describes our attitude determination method. Section 3 describes the array-aided positioning method. Section 4 presents real data analyses demonstrating the improved performance of the proposed methods. Finally, Section 5 contains the summary and conclusions of this contribution.

2 Attitude Determination

This section describes the platform processing involving attitude determination for a small-sized array of GNSS receivers/antennas with known local body frame antenna geometry. First the multibaseline attitude model is introduced using the multivariate formulation of [5]. This formulation makes a frequent use of the Kronecker product \otimes and the vec-operator [13]. Then we include the local body frame antenna-geometry and show how the constrained attitude model can be solved in a step-wise manner.

2.1 The multivariate model

Let us consider the k th platform equipped with a set of $n_k + 1$ antennas simultaneously tracking $m + 1$ satellites on f frequencies. The set of linearized Double Difference (DD) GNSS phase and code observations obtained on the n_k baselines formed by these antennas at an observation epoch forms a *multivariate* Gauss-Markov model [5, 11]:

$$E(Y^k) = AZ^k + GB^k, \quad Z^k \in \mathbb{Z}^{fm \times n_k}, B^k \in \mathbb{R}^{3 \times n_k} \quad (1)$$

$$D(\text{vec}(Y^k)) = Q_{y^k y^k} = P_{n_k} \otimes Q_{yy} \quad (2)$$

where $E(\cdot)$ and $D(\cdot)$ denote the expectation and dispersion operator, \otimes denotes the Kronecker product, $Y^k = [y_1^k, \dots, y_{n_k}^k]$ is the $2fm \times n_k$ matrix of n_k linearized (observed-minus-computed) DD observation vectors y_r^k , $Z^k = [z_1^k, \dots, z_{n_k}^k]$ is the $fm \times n_k$ matrix of n_k unknown DD integer ambiguity vectors z_j^k , $B^k = [b_1^k, \dots, b_{n_k}^k]$ the $3 \times n_k$ matrix of n_k unknown baseline vectors b_j^k , G is the $2fm \times 3$ geometry matrix that contains the unit line-of-sight vectors, A is the $2fm \times fm$ matrix that links the DD data to the integer ambiguities, and P_{n_k} and Q_{yy} are known matrices of order $n_k \times n_k$ and $2fm \times 2fm$, respectively. Here, $\text{vec}(\cdot)$ denotes the vec-operator, which transforms a matrix into a vector by stacking the columns of the matrix one underneath the other. Note that, for the simplicity of the formulation, we assumed that all receivers/antennas track the same set of satellites. However, this restriction is relaxed in the software implemented using Matlab. Since the unit line-of-sight vectors of two antennas to the same satellite on short

baselines considered in this work are the same for all practical purposes, the geometry matrix G is considered identical for different platforms as well as for between-platform baseline at a given time instant.

For the stochastic model, we assumed that all receivers/antennas have similar (noise) characteristics. However, the results in the following are also applicable for dissimilar receivers/antennas [11]. The correlation matrix P_{n_k} takes care of the correlation that follows from the fact that the n_k baselines share the observations from a reference receiver. For similar receivers/antennas, it is given as

$$P_{n_k} = \frac{1}{2} (I_{n_k} + e_{n_k} e_{n_k}^T) \quad (3)$$

with I_{n_k} the identity matrix of size n_k and e_{n_k} the n_k -vector of ones. Matrix Q_{yy} takes care of the precision of the phase and code data and is given as

$$Q_{yy} = \text{blockdiag}(Q_1, \dots, Q_f) \quad (4)$$

where

$$Q_f = 2 \times \text{blockdiag}(Q_{f:p}, Q_{f:\phi}) \quad (5)$$

$$Q_{f:p} = D_m^T Q'_{f:p} D_m \quad (6)$$

$$Q_{f:\phi} = D_m^T Q'_{f:\phi} D_m \quad (7)$$

$$Q'_{f:t} = \text{diag} \left[(\sigma_{f:t}^1)^2, \dots, (\sigma_{f:t}^{m+1})^2 \right], \quad (8)$$

with $D_m^T = [-e_m \ I_m]$ the single difference operator, ‘blockdiag’ referring to the block diagonal matrix formed by given arguments and ‘diag’ referring to the diagonal matrix formed by given arguments. The factor 2 in (5) is due to between-receiver difference of similar receivers. We assume elevation-dependent noise characteristics [14] for the undifferenced observables. That is, the standard deviation of the undifferenced observable can be written as:

$$\sigma_{f:t}^s = \sigma_{f:t_0} \left(1 + a_0 \exp \left(\frac{-\theta^s}{\theta_0} \right) \right) \quad (9)$$

where θ^s is the elevation angle of satellite s and $\sigma_{f:t_0}$, $a_{f:t_0}$ and $\theta_{f:t_0}$ are the elevation-dependent model parameters for type t (phase or code) observation at frequency f .

2.2 The body-frame antenna-geometry as multivariate constraints

The strength of the above model can be improved by including information about the geometry of the antenna

configuration. The known body-frame antenna-geometry can be included into the above model through the parametrization

$$B^k = R^k B_0^k, \quad R^k \in \mathbb{O}^{3 \times q_k} \quad (10)$$

with the unknown $3 \times q_k$ orthogonal matrix R^k ($R^{kT} R^k = I_{q_k}$), $\mathbb{O}^{3 \times q_k}$ denoting the set of orthogonal matrices of size $3 \times q_k$, and the known $q_k \times n_k$ matrix $B_0^k = [b_{0,1}^k, \dots, b_{0,n_k}^k]$ describing the known geometry of the antenna configuration in the body frame. Here, q_k is the degree of geometrical independence of the GNSS baselines, for example, $q_k = 1$ for co-linearly installed antennas, $q_k = 2$ for co-planarly installed antennas, and $q_k = 3$ for antennas installed not in a single plane. For $q_k = 3$, R^k is related to the Euler attitude angles $\vartheta = [\phi \ \theta \ \psi]^T$ as follows:

$$R(\vartheta) = \begin{bmatrix} c_\theta c_\phi & -c_\psi s_\phi + s_\psi s_\theta c_\phi & s_\psi s_\phi + c_\psi s_\theta c_\phi \\ c_\theta s_\phi & c_\psi c_\phi + s_\psi s_\theta s_\phi & -s_\psi c_\phi + c_\psi s_\theta s_\phi \\ -s_\theta & s_\psi c_\theta & c_\psi c_\theta \end{bmatrix} \quad (11)$$

with ϕ the heading, θ the elevation, ψ the bank, and where $s_\alpha = \sin(\alpha)$ and $c_\alpha = \cos(\alpha)$. Note that for $q < 3$, only the first q columns of R are defined. For example, for a linear antenna array ($q = 1$) only the first column is defined and hence only heading and elevation are estimable. For $q > 1$ (an array with more than two antennas that are not in a straight line), all three angles are estimable.

Substitution of (10) into (1), leads to the constrained GNSS attitude model [11, 15]

$$E(Y^k) = AZ^k + GR^k B_0^k, \quad Z^k \in \mathbb{Z}^{fm \times n_k}, \quad R^k \in \mathbb{O}^{3 \times q_k} \quad (12)$$

$$D(\text{vec}(Y^k)) = Q_{y^k y^k} = P_{n_k} \otimes Q_{yy} \quad (13)$$

Our objective is to solve for the attitude matrix R^k in a least-squares sense, thereby taking the integer constraint on matrix $Z^k \in \mathbb{Z}^{fm \times n_k}$ and the orthonormality constraint on matrix $R^k \in \mathbb{O}^{3 \times q_k}$ into account. Hence, the least-squares minimization problem that will be solved reads

$$\min_{Z^k \in \mathbb{Z}^{fm \times n_k}, R^k \in \mathbb{O}^{3 \times q_k}} \left\| \text{vec} \left(Y^k - AZ^k - GR^k B_0^k \right) \right\|_{Q_{y^k y^k}}^2 \quad (14)$$

with $\|\cdot\|_Q^2 = (\cdot)^T Q^{-1}(\cdot)$. This is a mixed integer nonlinear least-squares problem that does not permit a closed-form solution. We now describe how (14) can be solved.

2.3 The real-valued float solution

The float solution is defined as the solution of (14) without the constraints. When we ignore the integer constraint on Z^k and the orthonormality constraint on R^k , the float solutions \hat{Z}^k and \hat{R}^k , and their variance-covariance matrices are obtained from solving the system of normal equations:

$$\begin{bmatrix} Q_{Z^k Z^k} & Q_{Z^k \hat{R}^k} \\ Q_{\hat{R}^k Z^k} & Q_{\hat{R}^k \hat{R}^k} \end{bmatrix}^{-1} \begin{bmatrix} \text{vec}(\hat{Z}^k) \\ \text{vec}(\hat{R}^k) \end{bmatrix} = \mathcal{A}_k^T Q_{y^k y^k}^{-1} \text{vec}(Y^k) \quad (15)$$

with

$$\begin{bmatrix} Q_{Z^k Z^k} & Q_{Z^k \hat{R}^k} \\ Q_{\hat{R}^k Z^k} & Q_{\hat{R}^k \hat{R}^k} \end{bmatrix} = \left(\mathcal{A}_k^T Q_{y^k y^k}^{-1} \mathcal{A}_k \right)^{-1} \quad (16)$$

$$\mathcal{A}_k = \begin{bmatrix} I_{n_k} \otimes A^T \\ B_0^k \otimes G^T \end{bmatrix}^T \quad (17)$$

The Z^k -constrained solution of R^k and its variance-covariance matrix can be obtained from the float solution as follows

$$\text{vec}(\hat{R}^k(Z^k)) = \text{vec}(\hat{R}^k) - Q_{\hat{R}^k Z^k} Q_{Z^k Z^k}^{-1} \text{vec}(\hat{Z}^k - Z^k) \quad (18)$$

$$Q_{\hat{R}^k(Z^k) \hat{R}^k(Z^k)} = Q_{\hat{R}^k \hat{R}^k} - Q_{\hat{R}^k Z^k} Q_{Z^k Z^k}^{-1} Q_{Z^k \hat{R}^k} \quad (19)$$

Using the above estimators, the original problem in (14) can be decomposed as

$$\begin{aligned} & \min_{Z^k \in \mathbb{Z}^{fm \times n_k}, R^k \in \mathbb{O}^{3 \times q_k}} \left\| \text{vec} \left(Y^k - AZ^k - GR^k B_0^k \right) \right\|_{Q_{y^k y^k}}^2 \\ &= \left\| \text{vec}(\hat{E}^k) \right\|_{Q_{y^k y^k}}^2 + \min_{Z^k \in \mathbb{Z}^{fm \times n_k}} \left(\left\| \text{vec}(\hat{Z}^k - Z^k) \right\|_{Q_{Z^k Z^k}}^2 \right. \\ & \quad \left. + \min_{R^k \in \mathbb{O}^{3 \times q_k}} \left\| \text{vec}(\hat{R}^k(Z^k) - R^k) \right\|_{Q_{\hat{R}^k(Z^k) \hat{R}^k(Z^k)}}^2 \right) \end{aligned} \quad (20)$$

with $\hat{E}^k = Y^k - A\hat{Z}^k - G\hat{R}^k B_0^k$ being the matrix of least-squares residuals. Note that the first term on the right hand side is constant, as it does not depend on the unknown matrices Z^k and R^k .

2.4 The integer ambiguity solution

Based on the orthogonal decomposition (20), the multivariate constrained integer minimization can be formulated as:

$$\hat{Z}^k = \arg \min_{Z^k \in \mathbb{Z}^{fm \times n_k}} C^k(Z^k) \quad (21)$$

where

$$C^k(Z^k) = \left\| \text{vec}(\hat{Z}^k - Z^k) \right\|_{Q_{\hat{Z}^k Z^k}}^2 + \left\| \text{vec}(\hat{R}^k(Z^k) - \check{R}^k(Z^k)) \right\|_{Q_{\hat{R}^k(Z^k) \check{R}^k(Z^k)}}^2 \quad (22)$$

with

$$\check{R}^k(Z^k) = \arg \min_{R^k \in \mathbb{O}^{3 \times q_k}} \left\| \text{vec}(\hat{R}^k(Z^k) - R^k) \right\|_{Q_{\hat{R}^k(Z^k) \check{R}^k(Z^k)}}^2 \quad (23)$$

The ambiguity objective function $C^k(Z^k)$ is the sum of two coupled terms: the first weighs the distance from the float ambiguity matrix \hat{Z}^k to the nearest integer matrix Z^k in the metric of $Q_{\hat{Z}^k Z^k}$, while the second weighs the distance from the conditional float solution $\hat{R}^k(Z^k)$ to the nearest orthonormal matrix R^k in the metric of $Q_{\hat{R}^k(Z^k) \check{R}^k(Z^k)}$. Unlike with the standard LAMBDA method [16], the search space of the above integer minimization problem is non-ellipsoidal due to the presence of the second term in $C^k(Z^k)$. This second term is a consequence of having the orthonormality constraints rigorously included. The evaluation of $C^k(Z^k)$ requires the computation of a nonlinear constrained least-squares problem (23) for every integer matrix in the search space. In the MC-LAMBDA method, this problem is mitigated through the use of easy-to-evaluate bounding functions [8].

2.5 The ambiguity resolved attitude solution

Finally, we obtain the integer ambiguity resolved attitude solution by substituting \check{Z}^k into (18), thus giving $\hat{R}^k(\check{Z}^k)$. The sought-for attitude angles $\vartheta^k(\check{Z}^k)$ are then given by reparametrized solution of (23). Using a first order approximation, the formal variance-covariance matrix of the attitude angles is given by

$$Q_{\vartheta^k, \vartheta^k} \approx \left(J_{R^k, \vartheta^k}^T Q_{\hat{R}^k(Z^k) \check{R}^k(Z^k)}^{-1} J_{R^k, \vartheta^k} \right)^{-1} \quad (24)$$

where J_{R^k, ϑ^k} is the Jacobian of $\vartheta^k(R^k)$.

3 Integrated Positioning

This section describes the between-platform processing involving relative positioning between two platforms equipped with arrays of GNSS receivers/antennas. Array-aided positioning described in the following is a novel positioning concept improving between-platform positioning using array of antennas on the

platforms [10, 11]. First the combined observation model for all independent baselines among all receivers on both platforms is described. Then we describe attitude-bootstrapping showing how platform arrays improve the between-platform baseline estimate.

Let us consider two platforms carrying $n_1 + 1$ and $n_2 + 1$ receivers/antennas. The functional and stochastic models for the between-platform baseline formed by the first antennas (pivot antennas) read

$$E(y^{12}) = Az^{12} + Gb^{12} \quad z^{12} \in \mathbb{Z}^{fm} \quad (25)$$

$$D(y^{12}) = Q_{yy} \quad (26)$$

where y^{12} is the vector of between-platform double difference observables, z^{12} is the unknown vector of between-platform double difference ambiguities, and b^{12} is the unknown between-platform baseline. Note that atmosphere delays are not present in this formulation as we considered only sufficiently short baselines in the following. However, these atmosphere delays must be taken into account for general long baseline scenarios [11]. In standard positioning, the LAMBDA method yields the optimal estimates for the ambiguities and hence for baseline.

3.1 Array-aided Between-Platform Model:

By combining between-platform observables in (25) and platform array observables in (12), the functional and stochastic models of the integrated system read

$$E(\mathcal{Y}) = AZ + G\mathcal{R}B_0 \quad (27)$$

$$D(\text{vec}(\mathcal{Y})) = P \otimes Q_{yy} \quad (28)$$

where $\mathcal{Y} = [Y^1 \ Y^2 \ y^{12}]$ is the combined observation matrix, $\mathcal{R} = [R^1 \ R^2 \ b^{12}] \in \mathbb{R}^{3 \times (q_1 + q_2 + 1)}$ is the combination of rotation matrices and between-platform baseline, $Z = [Z^1 \ Z^2 \ z^{12}] \in \mathbb{Z}^{fm \times n_t}$ is the combined ambiguity matrix with $n_t = n_1 + n_2 + 1$, $B_0 = \text{blockdiag}(B_0^1, B_0^2, 1)$ is the combined local geometry matrix, and

$$P = \begin{bmatrix} P_{n_1} & 0 & \frac{1}{2}e_{n_1} \\ 0 & P_{n_2} & -\frac{1}{2}e_{n_2} \\ \frac{1}{2}e_{n_1}^T & -\frac{1}{2}e_{n_2}^T & 1 \end{bmatrix} \quad (29)$$

is the combined correlation matrix. The above system consists of attitude models of both platforms with unknowns Z^k and R^k , and a between-platform baseline model with unknowns z^{12} and b^{12} . Even though these three subsystems do not have any parameter in common,

they are correlated as in (29) due to the use of common observations from pivot antennas.

3.2 Array-aided Positioning

A-PPP method [11] uses a decorrelation technique to decouple the combined system in (27) such that the subsystems still yield the optimal solution. Using decorrelation matrix

$$\mathcal{D} = \begin{bmatrix} I_{n_1} & 0 & 0 \\ 0 & I_{n_2} & 0 \\ -\frac{1}{2}e_{n_1}^T P_{n_1}^{-1} & \frac{1}{2}e_{n_2}^T P_{n_2}^{-1} & 1 \end{bmatrix} \otimes I_{2fm} \quad (30)$$

the decorrelated system reads

$$E(\mathcal{Y}') = AZ' + G\mathcal{R}'B_0 \quad (31)$$

$$D(\text{vec}(\mathcal{Y}')) = P' \otimes Q_{yy} \quad (32)$$

where $\mathcal{Y}' = [Y^1 \ Y^2 \ y'^{12}]$ is the decorrelated observation matrix, $\mathcal{R}' = [R^1 \ R^2 \ b'^{12}] \in \mathbb{R}^{3 \times (q_1 + q_2 + 1)}$ is the combination of rotation matrices and between-platform baseline after decorrelation, $Z' = [Z^1 \ Z^2 \ z'^{12}]$ is the combined ambiguity matrix after decorrelation, and

$$P' = \text{blockdiag}(P_{n_1}, P_{n_2}, \eta) \quad (33)$$

with

$$y'^{12} = y^{12} - \frac{1}{n_1 + 1} \sum_{r=1}^{n_1} y_r^1 + \frac{1}{n_2 + 1} \sum_{r=1}^{n_2} y_r^2 \quad (34)$$

$$z'^{12} = z^{12} - \frac{1}{n_1 + 1} \sum_{r=1}^{n_1} z_r^1 + \frac{1}{n_2 + 1} \sum_{r=1}^{n_2} z_r^2 \quad (35)$$

$$b'^{12} = b^{12} - \frac{1}{n_1 + 1} R^1 \sum_{r=1}^{n_1} b_{0,r}^1 + \frac{1}{n_2 + 1} R^2 \sum_{r=1}^{n_2} b_{0,r}^2 \quad (36)$$

$$\eta = \frac{n_t + 1}{2(n_1 + 1)(n_2 + 1)} \quad (37)$$

This decorrelation keeps the platform processing intact as in (21) and only alters the between-platform model. As a result of decorrelation, the ambiguities in (35) may not be integer. However, once platform ambiguities are determined reliably using MC-LAMBDA with decoupled platform models in (31), the model for the between-platform baseline can be rearranged as

$$E(y''^{12}) = Az^{12} + Gb'^{12} \quad z^{12} \in \mathbb{Z}^{fm} \quad (38)$$

$$D(y''^{12}) = \eta Q_{yy} \quad (39)$$

where

$$y''^{12} = y'^{12} + \frac{1}{n_1 + 1} \sum_{r=1}^{n_1} Az_r^1 - \frac{1}{n_2 + 1} \sum_{r=1}^{n_2} Az_r^2 \quad (40)$$

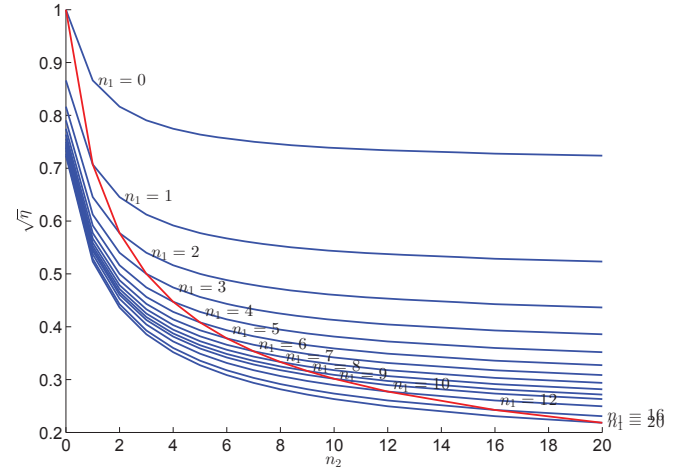


Figure 1. Noise reduction factor ($\sqrt{\eta}$) due to array-aided positioning with $n_1 + 1$ antennas on the reference platform and $n_2 + 1$ antennas on the rover platform; the red curve corresponds to both platforms having equal number of antennas

Due to the reduction of variance-covariance by a factor of η , this model yields improved ambiguity resolution and baseline estimation compared to the standard positioning model in (25). That is, the use of array-aided positioning reduces the variance-covariance matrices of the float ambiguities and ambiguity fixed baseline estimators by a factor of η . Figure 1 depicts the noise reduction ($\sqrt{\eta}$) due to array-aided positioning as a function of n_1 and n_2 . The red curve corresponds to both platforms having equal number of antennas. Note that the between-platform baseline estimate in (36) corresponds to the vector between the centroids of the antenna arrays. The unconstrained mixed integer least-squares problem defined in (38) and (39) can be solved efficiently using LAMBDA method [16] providing ambiguity-fixed baseline estimate $\check{b}'^{12}(\check{z}')$ and associated variance-covariance matrix $Q_{\check{b}'^{12}(\check{z}')\check{b}'^{12}(\check{z}'})$.

4 Real-Data Analysis

In this section the performance analyses of the proposed attitude determination and array-aided positioning methods are presented. Data sets from two measurement campaigns are used to demonstrate the improved performance of the proposed methods. The stochastic model parameters of the elevation dependent model (7) for these data sets are reported in Table 1. The performance measures include the empirical instantaneous ambiguity resolution success rate, and the

	$\sigma_{f:t_0}$
Code [cm]	30
Phase [mm]	20

Table 1. Elevation-dependent stochastic model parameters with $a_0 = 5$ and $\theta_0 = 20$ defined in (9)



Figure 2. Arrays of five antennas used in the experiment setup at Delft University of Technology (20 m baseline)

position and angular accuracy given by their root mean squared error (RMSE).

4.1 Experiment I

This experiment was conducted at Delft University of Technology on September 6, 2010 with two platforms (arrays) placed about 20 m apart. As shown in Figure 2, each array consists of three Trimble Zephyr and two Trimble Zephyr Geodetic antennas connected to five Trimble R7 receivers. GPS data was collected at a rate of 1 Hz for about 2 hours (6250 epochs). Results from single-frequency, epoch-by-epoch processing of this data set are discussed in the following.

Table 2 summarizes the ambiguity resolution success rate of the platform processing (attitude determination) using the MC-LAMBDA method compared to the standard LAMBDA method. Making use of the known antenna geometry in the local body frame, the MC-LAMBDA method yields a high success rate even under the simulated satellite deprived (masking) environment. Table 3 reports attitude angular RMSE indicating slight degradation of angular accuracy with elevation cut-off angle.

Figure 3 depicts the baseline scatter plots for

Elevation Cut-off [deg]	LAMBDA	MC-LAMBDA
10	99.9	100
20	71.7	100
30	2.5	79.5

Table 2. Instantaneous ambiguity resolution success rate [%] for platform processing of the data from Delft experiment

Elevation [deg]	Cut-off	Heading	Elevation	Bank
10		0.03	0.08	0.13
20		0.03	0.08	0.16
30		0.05	0.12	0.19

Table 3. Ambiguity-fixed attitude accuracy (angular RMSE [deg]) for platform processing of the data from Delft experiment:

between-platform processing comparing the performance of the proposed array-aided real-time kinematic (RTK) positioning with that of the standard RTK positioning. It also summarizes the position RMSE values of both methods demonstrating the noise reduction for array-aided RTK with five antennas per platform by a factor of about 0.38 matching the theoretical gain of $\frac{1}{\sqrt{5}}$ (Figure 1). Since the standard RTK positioning using single-frequency GPS data with elevation cut-off angle of 10° already yields instantaneous ambiguity resolution, we consider a high elevation cut-off angle (20°) to demonstrate the benefits of array-aided RTK positioning under satellite deprived (masking) environment. Figure 4 depicts the impact of number of antennas/receivers on array-aided RTK positioning using single-frequency GPS data with 20° elevation cut-off demonstrating improved ambiguity resolution and position estimation with number of receivers/antennas.

4.2 Experiment II

This experiment was conducted in Perth, Australia on September 12, 2013 with two platforms (arrays) placed about 4.3 km apart. As shown in Figure 5, each platform was equipped with four Javad JAV_GRANT-G3T antennas connected to four Javad TRE_G3T DELTA receivers and collecting GPS+BeiDou data for about 12 hours with a sampling interval of 10 s. For this multi-system data, we considered a multi-system formulation [17] of the multi-variate system of equation in (1). Since one of the receivers malfunctioned due to wrong configuration, results of array-aided RTK positioning using three antennas per platform are discussed in the following.

Table 4 summarizes the ambiguity resolution success rate for platform processing (attitude determination) for the Perth experiment demonstrating improved performance of the MC-LAMBDA method compared to that of the standard LAMBDA method. The

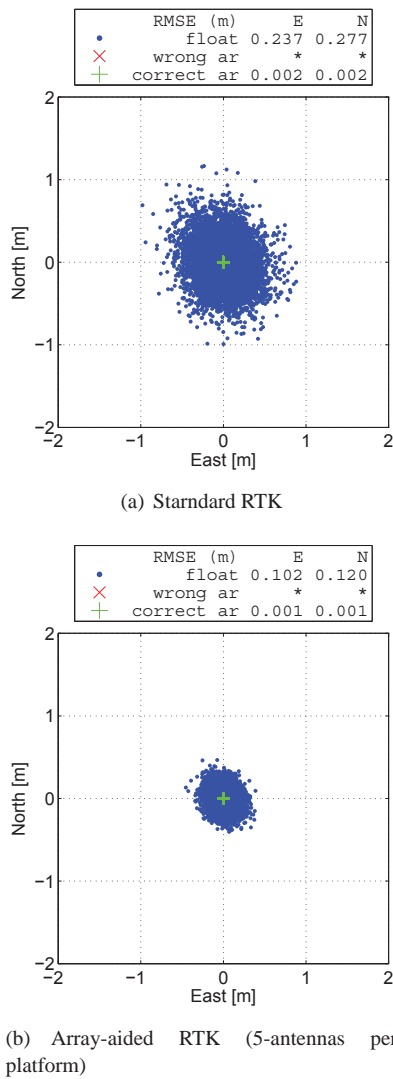


Figure 3. North-East scatter-plot for 20 m baseline using GPS single-frequency (L1) processing with elevation cut-off of 10°

MC-LAMBDA method yields instantaneous ambiguity resolution even under severe satellite deprived (masking) environment. Furthermore, the use of multi-system, multi-frequency processing increases the reliability of ambiguity resolution. Table 5 reports ambiguity-fixed attitude accuracy (angular RMSE) indicating slightly improved angular accuracy due to the use of multi-system, multi-frequency processing.

Table 6 reports the ambiguity resolution success rate for between platform processing for the Perth experiment demonstrating improved performance of the array-aided RTK method compared to that of the standard RTK method. Figures 6 - 8 depict baseline scatter plots for

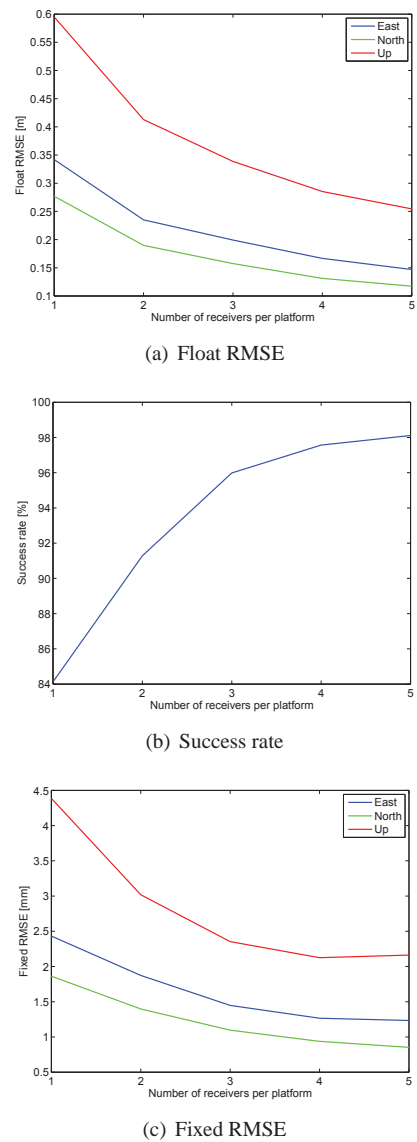


Figure 4. The performance of array-aided positioning with number of receivers (Delft experiment, 20 m): Single-frequency, atmosphere-fixed processing with 20° elevation cut-off

between-platform processing of Perth data (4.3 km baseline) indicating noise reduction due to the use of antenna arrays. Furthermore, the use of multi-system, multi-frequency processing improves between-platform ambiguity resolution and baseline estimation accuracy.

5 Conclusions

In this contribution we analysed the performance of attitude determination and array-aided relative positioning using GNSS data from two measurement



(a) Curtin University



(b) South Perth

Figure 5. Antenna setup for 4.3 km baseline experiment in Perth, Australia

System (Frequency)	Elevation Cut-off [deg]	LAMBDA	MC-LAMBDA
GPS (L1)	10	84.3	100
	30	13.6	91.6
	50	0.0	11.5
BeiDou (B1)	10	90.2	100
	30	32.3	99.7
	50	0.0	28.2
GPS (L1) + BeiDou (B1)	10	100	100
	30	99.7	100
	50	18.6	92.1
GPS (L1-L2)	10	100	100
	30	98.5	100
	50	23.3	29.9
BeiDou (B1-B2)	10	100	100
	30	100	100
	50	40.5	65.3
GPS (L1-L2) + BeiDou (B1-B2)	10	100	100
	30	100	100
	50	96.4	98.3

Table 4. Instantaneous ambiguity resolution success rate [%] for platform processing (attitude determination) of Perth Experiment

System (Frequency)	Heading	Elevation	Bank
GPS (L1)	0.09	0.31	0.36
BeiDou (B1)	0.08	0.25	0.33
GPS (L1) + BeiDou (B1)	0.06	0.20	0.24
GPS (L1-L2)	0.07	0.26	0.30
BeiDou (B1-B2)	0.07	0.21	0.26
GPS (L1-L2) + BeiDou (B1-B2)	0.05	0.18	0.20

Table 5. Ambiguity-fixed attitude accuracy for platform processing of Perth Experiment : angular RMSE [deg]

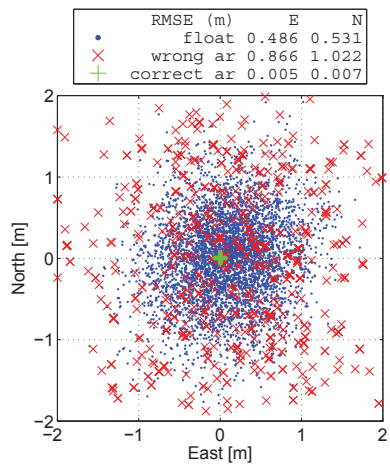
System (Frequency)	Elevation Cut-off [deg]	Standard RTK	Array-aided RTK (3-antennas per platform)
GPS (L1)	10	82.4	94.3
	30	26.8	47.4
	50	0.4	1.0
BeiDou (B1)	10	93.4	98.1
	30	49.8	71.0
	50	0.3	2.0
GPS (L1) + BeiDou (B1)	10	100	100
	30	99.9	100
	50	30.4	52.2
GPS (L1-L2)	10	100	100
	30	99.5	100
	50	30.1	31.2
BeiDou (B1-B2)	10	100	100
	30	99.9	100
	50	55.8	62.7
GPS (L1-L2) + BeiDou (B1-B2)	10	100	100
	30	100	100
	50	97.3	98.1

Table 6. Instantaneous ambiguity resolution success rate [%] for between-platform processing of Perth Experiment: 4.3 km baseline

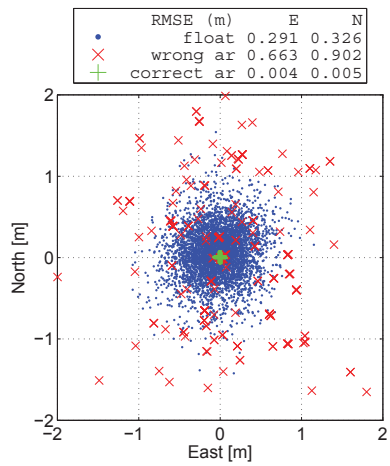
campaigns. The use of a known antenna geometry for platform processing (MC-LAMBDA) enhances platform ambiguity resolution especially in the case of single-frequency processing and under satellite deprived conditions. We have also demonstrated that array-aided relative positioning effectively utilized the reliable platform ambiguity resolution from the MC-LAMBDA method to improve between-platform processing in terms ambiguity resolution and baseline accuracy. Furthermore, the use of multi-system, multi-frequency processing enhances the performance of both platform processing and between-platform processing.

Acknowledgements

This work has been executed as part of the Positioning Program Project 1.01 New carrier phase processing strategies for achieving precise and reliable multi-satellite, multi-frequency GNSS/RNSS positioning in Australia of the Cooperative Research Centre for Spatial Information (CRC-SI). The second author P. J. G. Teunissen is the recipient of an Australian Research Council Federation Fellowship (project number FF0883188). All this support is gratefully acknowledged.



(a) Standard RTK

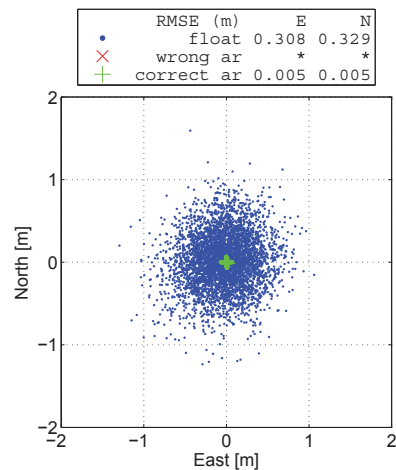


(b) Array-aided RTK (3-antennas per platform)

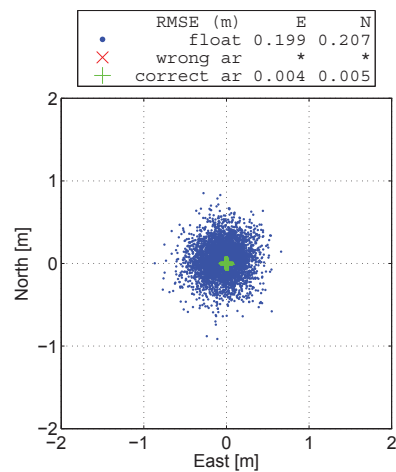
Figure 6. North-East scatter-plot for 4.3 km baseline using GPS single-frequency (L1) processing with elevation cut-off of 10°

References

- [1] M. O'Connor, T. Bell, G. Elkaim, and B. Parkinson, "Automatic steering of farm vehicles using GPS," in *Precision Agriculture*, P. Robert, R. Rust, and W. Larson, Eds. American Society of Agronomy, Crop Science Society of America, Soil Science Society of America, 1996, ch. 3, pp. 767–777.
- [2] D. Diefes, "GPS based attitude determining system for marine navigation," in *IEEE Position Location and Navigation Symposium*, Apr 1994, pp. 806–812.
- [3] R. J. Ray, B. R. Cobleigh, M. J. Vachon, and C. StJohn, "Flight test techniques used to evaluate



(a) Standard RTK

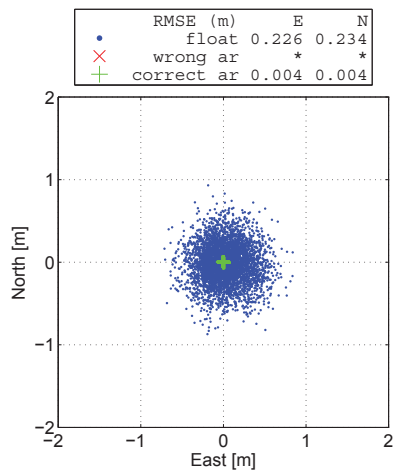


(b) Array-aided RTK (3-antennas per platform)

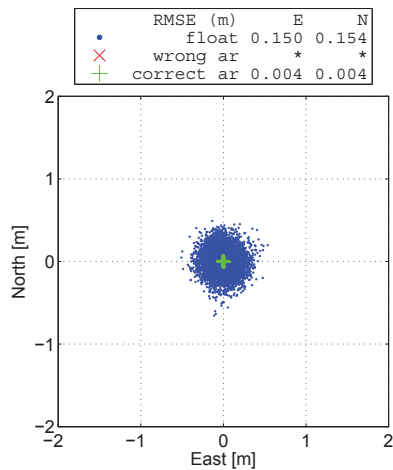
Figure 7. North-East scatter-plot for 4.3 km baseline using GPS dual-frequency (L1-L2) processing with elevation cut-off of 10°

performance benefits during formation flight," NASA Dryden Research Center, Edwards, CA, Tech. Rep. TP-2002-210730, 2002.

- [4] S. D'Amico and O. Montenbruck, "Differential GPS: An enabling technology for formation flying satellites," in *Small Satellite Missions for Earth Observation*, R. Sandau, H.-P. Roeser, and A. Valenzuela, Eds. Springer Berlin Heidelberg, 2010, pp. 457–465.
- [5] P. J. G. Teunissen, "A general multivariate formulation of the multi-antenna GNSS attitude determination problem," *Artificial Satellites*, vol. 42, no. 2, pp. 97–111, 2007.



(a) Standard RTK



(b) Array-aided RTK (3-antennas per platform)

Figure 8. North-East scatter-plot for 4.3 km baseline using dual-system (GPS+BeiDou), dual-frequency (L1-L2/B1-B2) processing with elevation cut-off of 10°

[6] G. Giorgi, P. J. G. Teunissen, S. Verhagen, and P. J. Buist, "Testing a new multivariate GNSS carrier phase attitude determination method for remote sensing platforms," *Advances in Space Research*, vol. 46, no. 2, pp. 118 – 129, 2010.

[7] N. Nadarajah, P. J. G. Teunissen, and N. Raziq, "Instantaneous GPS-Galileo attitude determination: single-frequency performance in satellite-deprived environments," *IEEE Transactions on Vehicular Technology*, vol. 62, no. 7, pp. 2963–2976, September 2013.

[8] N. Nadarajah, P. J. G. Teunissen, and G. Giorgi,

"GNSS attitude determination for remote sensing: On the bounding of the multivariate ambiguity objective function," in *Earth on the Edge: Science for a Sustainable Planet*, ser. International Association of Geodesy Symposia, C. Rizos and P. Willis, Eds. Springer Berlin Heidelberg, 2014, vol. 139, pp. 503–509.

[9] N. Nadarajah, P. J. Teunissen, and N. Raziq, "Instantaneous BeiDou-GPS attitude determination: A performance analysis," *Advances in Space Research*, vol. 54, no. 5, pp. 851 – 862, 2014, recent progresses on Beidou/COMPASS and other Global Navigation Satellite Systems (GNSS) - {II}.

[10] P. J. Buist, P. J. G. Teunissen, S. Verhagen, and G. Giorgi, "A vectorial bootstrapping approach for integrated GNSS-based relative positioning and attitude determination of spacecraft," *Acta Astronautica*, vol. 68, no. 7-8, pp. 1113 – 1125, 2011.

[11] P. J. G. Teunissen, "A-PPP: array-aided precise point positioning with global navigation satellite systems," *IEEE Transactions on Signal Processing*, vol. 60, no. 6, pp. 2870 – 2881, June 2012.

[12] N. Nadarajah, J.-A. Paffenholz, and P. J. G. Teunissen, "Integrated GNSS attitude determination and positioning for direct georeferencing," *Sensors*, vol. 14, no. 7, pp. 12715–12734, 2014.

[13] D. A. Harville, *Matrix Algebra From A Statistician's Perspective*. New York: Springer, 1997.

[14] H.-J. Euler and C. Goad, "On optimal filtering of GPS dual frequency observations without using orbit information," *Journal of Geodesy*, vol. 65, pp. 130–143, 1991.

[15] G. Giorgi, P. J. G. Teunissen, S. Verhagen, and P. J. Buist, "Instantaneous ambiguity resolution in Global-Navigation-Satellite-System-based attitude determination applications: a multivariate constrained approach," *Journal of Guidance, Control, and Dynamics*, vol. 35, no. 1, pp. 51–67, 2012.

[16] P. J. G. Teunissen, "The least-squares ambiguity decorrelation adjustment: a method for fast GPS

integer ambiguity estimation,” *Journal of Geodesy*, vol. 70, pp. 65–82, 1995.

- [17] N. Nadarajah, P. J. G. Teunissen, P. J. Buist, and P. Steigenberger, “First results of instantaneous GPS/Galileo/COMPASS attitude determination,” in *Proceedings of the 6th ESA Workshop on Satellite Navigation User Equipment Technologies (NAVITEC’12)*, Noordwijk, The Netherlands, 5-7 December 2012, pp. 1–8.